arXiv:1302.7108v1 [cond-mat.mes-hall] 28 Feb 2013

Theory of giant magnetoresistance at misfit interfaces

Daichi Asahi[1] and Naoto Nagaosa[1,2]
[1]Department of Applied Physics, University of Tokyo, Tokyo 113-8656, Japan
[2]RIKEN Center for Emergent Matter Science, ASI, RIKEN, Wako 351-0198, Japan

(Dated: March 1, 2013)

We study theoretically the resistance at the interface between the two planar systems with different lattice constants a and b. The resistance and the effect of the magnetic field depends sensitively on the ratio a/b. The size of the enlarged unit cell $\lambda = n_A a = n_B b$ (n_A, n_B: integers) is the crucial quantity, and the magnetic flux penetrating this enlarged unit cell determines the oscillation of the resistance. Therefore, the magnetoresistance is very much enhanced at (nearly) incommensurate relation between a and b.

PACS numbers: 74.20.-z, 74.62.Dh, 71.10.Pm
Keywords: giant magnetoresistance, misfit, incommensurability

Interfaces between different materials are the sources of rich physics and functions. Novel phenomena emerge that are not expected from each of the constituents [1]. One example is a two dimensional metallic state appearing at the interface between two insulators $LaAlO_3$ and $SrTiO_3$ [2]. Even superconductivity appears in this two-dimensional system, which is an issue of recent intensive interests [1]. Another example is the tunneling magnetoresistance (TMR) [3]. The resistance across the interface between the two ferromagnets depends strongly on the relative direction of the magnetizations. Therefore, transport properties perpendicular to the interface offer many useful functions for applications.

An essential nature of interfaces between different systems is the misfit of the lattice constants, which often causes the distortion of the lattice structure to relax this misfit when it is not so large. In this case, the lattice constants slowly change from the interface to the bulk region, and correspondingly electrons adiabatically follow this gradual change. When the misfit is larger, on the other hand, the system can not remedy this misfit and an incommensurate situation occurs at the interface.

Incommensurate systems attract recent attention from the viewpoints of charge/spin density waves [4], localization of wavefunctions [5], and quasi-crystals [6]. In these systems, incommensurability occurs in the bulk states, which is rather exceptional or special cases. On the other hand, the incommensurability occurs very often at interfaces since there is no definite relation between the lattice constants of the two systems.

In this paper, we study theoretically the tunneling conductance across the interface between the two two-dimensional systems A and B with lattice constants a and b, respectively. The ratio a/b matters significantly in this tunneling process, and also its sensitivity to an external magnetic field.

Let us start with the two one-dimensional chains A and B. The extension to two-dimensions is straightforward. We assume two chains have the same length L. The number of sites in chain A and in chain B are N_A and N_B, which are determined from $L = aN_A = bN_B$. We assume that two chains are parallel to x-direction with the separation c, and the tunneling amplitude between the nth site in chain A and the mth site in chain B is given by

$$t_{nm} = t_{AB} e^{iBc\frac{an+bm}{2}} \left(e^{-\frac{|an-bm|}{d}} + e^{-\frac{L-|an-bm|}{d}} \right). \quad (1)$$

Here d characterizes the spatial extent of the tunneling process. Two chains are placed in a magnetic field, which is perpendicular to the plane including two chains. The magnetic field induces AB phase (Aharanov-Bohm phase). We choose the gauge as $\boldsymbol{A} = (0, Bx)$.

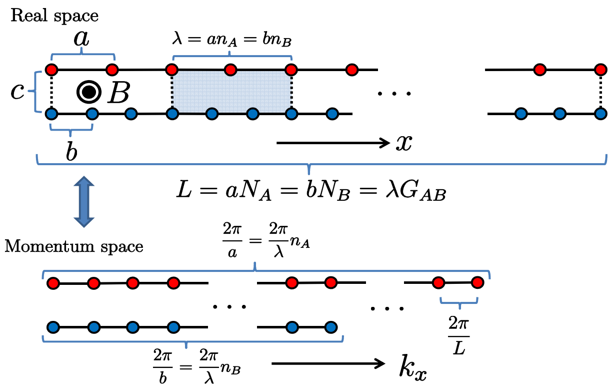

FIG. 1: The upper panel indicates two chains in the real space. One chain has the lattice constant a, and the other chain has the lattice constant b, which are placed in a magnetic field. The smallest periodic part is constructed from n_A sites of chain A and n_B sites of chain B, i.e., the size of the enlarged unit cell λ is given by $\lambda = an_A = bn_B$. G_{AB} is the number of this enlarged unit cell and hence is the greatest common divisor of N_A and N_B, i.e., $N_A = n_A G_{AB}$ and $N_B = n_B G_{AB}$, and $L = G_{AB}\lambda$. The bottom panel indicates the momentum space of chain A and chain B. The Brillouin zones of A and B are discretized by the same unit $2\pi/L$, while the sizes are different. The Brillouin zones are decomposed into n_A and n_B parts by $\frac{2\pi}{\lambda}$.

We rewrite Eq. (1) by wavenumber representation as

$$t_{kp}=\frac{1}{\sqrt{N_AN_B}}\sum_{nm}t_{nm}e^{-i\frac{2\pi k}{N_A}n+i\frac{2\pi p}{N_B}m}, \tag{2}$$

where the wavenumbers are specified by the integers k and p. The lattice constant λ of the composite system of A and B is given by $\lambda=an_A=bn_B$, where we define as $n_A=\frac{N_A}{G_{AB}}$ and $n_B=\frac{N_B}{G_{AB}}$. G_{AB} is the greatest common divisor of N_A and N_B, and is the number of the unit cells with the lattice constant λ, i.e., $L=G_{AB}\lambda$. The translational symmetry by $\lambda\boldsymbol{e}_x$ leads to the conservation of wave numbers by mod $\frac{2\pi}{\lambda}$. The Brillouin zones are decomposed into n_A and n_B parts by $\frac{2\pi}{\lambda}$.

The summations in Eq. (2) can be carried out (See in the appendix) and t_{kp} is obtained as

$$t_{kp}=\frac{G_{AB}}{\sqrt{N_AN_B}}\delta_{G_{AB}}\left(k-p-2M\right)f\left(k-M,p+M\right) \tag{3}$$

$$f\left(k,p\right)=\frac{\left(1-e^{-\frac{L}{d}}\right)\sinh\left(\frac{\xi}{d}\right)}{\cosh\left(\frac{\xi}{d}\right)-\cos\left(\frac{2\pi x_A}{N_A}k-\frac{2\pi x_B}{N_B}p\right)}. \tag{4}$$

$\delta_{G_{AB}}$ is defined as

$$\delta_{G_{AB}}\left(k-p\right)=\begin{cases}1 & k-p=0 \mod G_{AB}\\ 0 & \text{otherwise.}\end{cases} \tag{5}$$

Equation (5) represents the wavenumber conservation. ξ is the characteristic length of this system, which is represented as $\xi=\frac{L}{L_{AB}}=\frac{b}{n_A}=\frac{a}{n_B}$. x_A and x_B are solutions of the Diophantine equation $n_Bx_A-n_Ax_B=1$. This equation has an integer solution because n_A and n_B are coprime. (x_A+mn_A,x_B+mn_B) is also the solution, where m is an arbitrary integer, but this indefiniteness is not concerned with Eq. (3) because of Eq. (5). Equation (4) represents the interference in the periodic part.

We consider the resistance at an interface between the two-dimensional systems A and B, which are the straightforward generalization of the above chain system. The conductance g per one enlarged unit cell is represented as

$$g=\frac{G}{G_{AB}^2}=\frac{1}{n_A^2n_B^2}\sum_{k_x,k_y=0}^{n_A-1}\sum_{p_x,p_y=0}^{n_B-1}\sigma_{\boldsymbol{kp}}^{n_An_B}(\boldsymbol{b}). \tag{6}$$

We take a limit $G_{AB}\to\infty$, and

$$\begin{aligned}\sigma_{\boldsymbol{kp}}^{n_An_B}(\boldsymbol{b})=&\int_0^1dx\int_0^1dyF\left(\boldsymbol{k}+\boldsymbol{x}+\frac{\boldsymbol{b}}{2},\boldsymbol{p}+\boldsymbol{x}+\frac{\boldsymbol{b}}{2}\right)\\ &\times\delta\left(\xi_A\left(\frac{2\pi}{n_A}\left(\boldsymbol{k}+\boldsymbol{b}+\boldsymbol{x}\right)\right)\right)\delta\left(\xi_B\left(\frac{2\pi}{n_B}\left(\boldsymbol{p}+\boldsymbol{x}\right)\right)\right).\end{aligned} \tag{7}$$

with

$$F(\boldsymbol{k},\boldsymbol{p})=\left|t_{AB}f_C\left(k_x,p_x\right)f_C\left(k_y,p_y\right)\right|^2 \tag{8}$$

$$f_C\left(k,p\right)=\frac{\sinh\left(\frac{\xi}{d}\right)}{\cosh\left(\frac{\xi}{d}\right)-\cos\left(\frac{2\pi x_A}{n_A}k-\frac{2\pi x_B}{n_B}p\right)}. \tag{9}$$

$\boldsymbol{b}$ is the dimensionless magnetic flux penetrating the enlarged unit cell, i.e., $\boldsymbol{B}c\lambda=2\pi\boldsymbol{b}$. The resistance R per the unit area is given by $R=\frac{\lambda^2}{g}$, which is the physical quantity of our main interest.

First, we study the lattice constant λ of the enlarged unit cell. $\frac{1}{\lambda}$ change radically as the ratio $\frac{a}{b}=\frac{n_B}{n_A}=\frac{N_B}{N_A}$. Particularly, $\frac{1}{\lambda}$ indicates a fractal architecture with fixed N_A, if N_A is a power of a prime number. We show this relation in Fig. 2 with the fixed lattice constant a of chain A. The upper left panel indicates the global behavior of $\frac{1}{\lambda}$ v.s. $\frac{a}{b}=\frac{N_B}{N_A}$, and the rest panels show the graphs for selected $\frac{N_B}{N_A}$ with fixed $N_A=2^{10},3^8,6^4$. When $N_A=2^{10},3^8$, it shows clear fractal structures, while it shows a complex structure when $N_A=6^4$. When $N_A=p^n$ where p is a prime number, $\frac{1}{\lambda}$ is given by the following calculations. We define $S_i=\left\{p^{n-i},2p^{n-i},\cdots\left(p^i-1\right)p^{n-i}\right\}$ $(i=1,2,\cdots n)$ and $P_i=S_i-S_{i-1}$ $(i=1,2,\cdots n)$, where we set $S_0=\phi$ (empty set). The relation between λ and $\frac{N_B}{N_A}$ is specified as

$$\frac{1}{\lambda}=\frac{1}{ap^i} \tag{10}$$

when $N_B\in P_i$. This relation and the definition of P_i generate the fractal structure scaled by $\frac{1}{p}$. When N_A is not a power of a prime number, this fractal structure is not there, but $\frac{1}{\lambda}$ shows a highly singular behavior as a function of $\frac{a}{b}$ as shown in panels (a) and (d) of Fig. 2.

Next, we consider the magnetic field dependence of R to see the proper scaling for $\boldsymbol{B}$. In a limiting case $d\to0$, the hopping amplitude is finite only between sites whose x-coordinates and y-coordinates are the same. In this limit, $F=1$ and it is clear that the resistivity has the period $\Delta b_i=1$, which is independent of (n_A,n_B). From $\boldsymbol{B}c\lambda=2\pi\boldsymbol{b}$, the resistivity of the misfit interface is enhanced for larger λ (or n_A,n_B), i.e., (nearly) incommensurate case. In this case, $\xi=\frac{a}{n_B}$ is small, so we cannot assume $\xi\gg d$. Then there is a crossover from $d\to0\ll\xi$ to $d\gg\xi$, and the interference in the periodic part F occurs in the latter case where the period of the conductivity becomes $\Delta b_i=2l_{AB}$, where l_{AB} is the least common multiple of n_A and n_B. However, as will be seen for explicit examples, the variation of R occurs within the scale of $\Delta b_i=1$ even for $d\gg\xi$.

We estimate the behavior of R with λ in the limiting cases. In a limiting case $d\to0$, one enlarged unit cell has one pair of sites connected by the finite hopping amplitude, and hence R grow as $\propto\lambda^2$. When $d\cong a\cong b$,

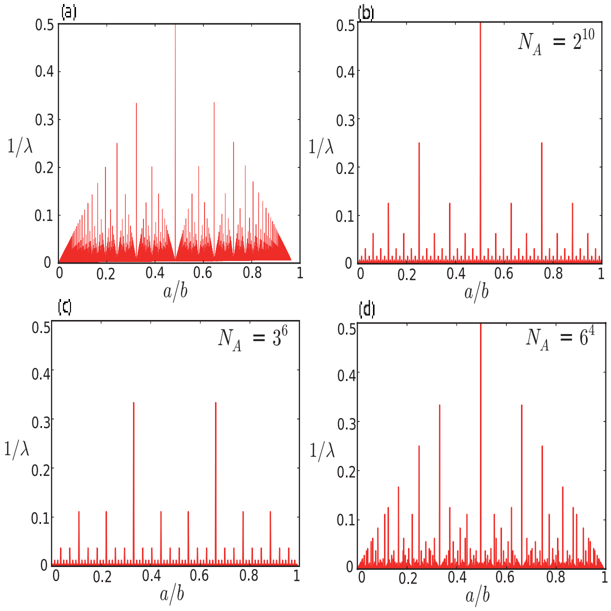

FIG. 2: The variation of $\frac{1}{\lambda}$ (λ the size of the enlarged unit cell) as a function of $\frac{a}{b} = \frac{N_B}{N_A}$: Panel (a) indicates the global behavior while the rest panels (b),(c), and (d) indicate $\frac{1}{\lambda}$ for selected $\frac{a}{b} = \frac{N_B}{N_A}$ with fixed $N_A = 2^{10}, 3^6$, and 6^4, respectively. When $N_A = 2^{10}, 3^6$, it show fractal structures, but it shows a complex structure when $N_A = 6^4$.

which is more relevant to the realistic systems, there are many finite hopping amplitudes between sites in one enlarged unit cell, and the number of site in each chain does not becomes important. The hopping amplitude per area does not change with λ and the scale of R is nearly constant although the magnetic field dependence is sensitive to λ. In the extreme case $a \ll b$, on the other hand, the situation is similar to the case of $d = 0$, and R is expected to grow with $\propto \lambda^2$.

Now, let us study a concrete example. We assume the simplest tight binding model on a square lattice both for A and B as $\epsilon_{A(B)}(\boldsymbol{k}) = \cos k_x + \cos k_y$ with the chemical potential at $\mu = 0$, and the magnetic field is along the x-axis, i.e., $b_y = 0$. From Eq. (6) and Eq. (7), we can obtain the analytic form of the conductivity as given in the appendix. In the following calculations, we fix the lattice constant of A as $a = 1$ and set $\frac{t_{AB}^2}{2\pi^2} = 1$.

In this model, the Fermi surfaces is straight line as indicated in Fig. 3. At the misfit interface, the Brillouin zone is reduced to $n_A \times n_A$ ($n_B \times n_B$) parts by $\frac{2\pi}{\lambda}$. The segmented pieces of the Fermi surfaces are determined by the parity of n_A (n_B). This even-odd effect is a special properties of the linear Fermi surfaces. In Fig. 3, we indicate two examples, i.e., cases of $n_A = 2$ and 3.

We now consider the resistance R as a function of the magnetic field B_x and the dimensionless magnetic flux b_x. The resistance R at $B_x = b_x = 0$ reflect the even-odd effect of the Fermi surfaces. When both n_A and n_B are odd, $R = 0$ for integer values of b_x. On the other hand, when either n_A or n_B is even, $R = 0$ at $b_x = \text{integer} + \frac{1}{2}$. Strictly speaking, $R = 0$ means the diverging g and hence the perturbation theory with respect to t_{AB} does not work there. This divergence has two origins, i.e., the Van Hove singularity and the fact that the forms of the Fermi surface of ϵ_A and ϵ_B are the same.

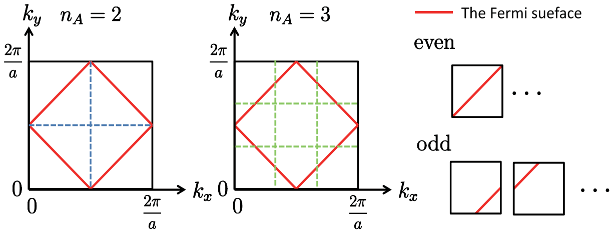

FIG. 3: The Fermi surface for $\epsilon_{A(B)}(\boldsymbol{k}) = \cos k_x + \cos k_y$: The Fermi surfaces are indicated by red lines. Due to the folding of the 1st Brillouine zone (BZ), the Fermi surface is segmented into smaller pieces in the reduced BZ, which depends on the parity of n_A (n_B). We show two examples $n_A = 2$ and 3 at the right panel for even and odd $n_A(n_B)$, respectively.

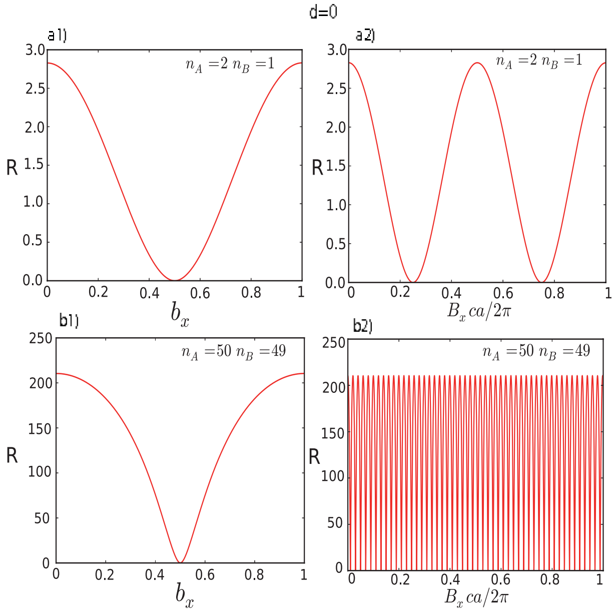

FIG. 4: Resistance per unit area R for $d = 0$: The panels (a1) and (b1) shows R as a function of b_x while (a2) and (b2) as a function of $\frac{B_x ac}{2\pi}$. Panels (a1) and (a2) are for $(n_A, n_B) = (2, 1)$, while (b1) and (b2) are for $(n_A, n_B) = (50, 49)$. R depends on the magnetic field through the flux penetrating the enlarged unit cell. and when λ is large, R oscillates as $\frac{B_x ac}{2\pi}$ more rapidly and the maximum value becomes larger as $\propto \lambda^2$ as shown in Fig.6(b1).

At first, we consider a limiting case $d \to 0$. The behavior of the resistance R depends on the parity of n_A and n_B, which reflects the even-odd effect of the Fermi

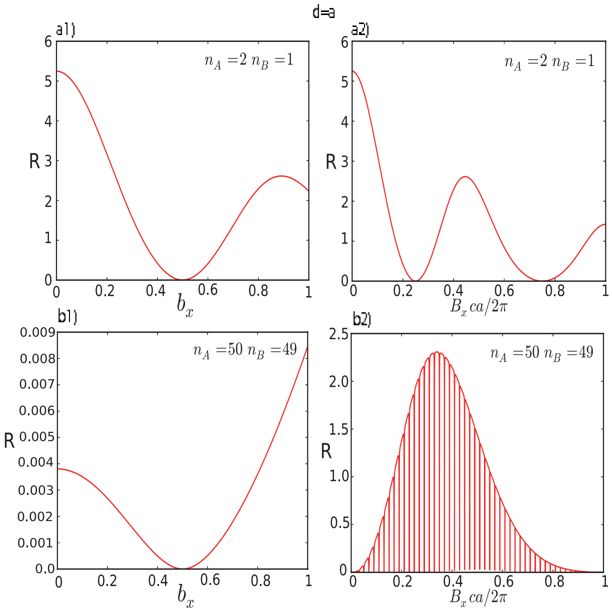

FIG. 5: Resistance per unit area R for $d = a$: The panels (a1) and (b1) shows R as a function of b_x while (a2) and (b2) as a function of $\frac{B_x ac}{2\pi}$. Panels (a1) and (a2) are for $(n_A, n_B) = (2, 1)$, while (b1) and (b2) are for $(n_A, n_B) = (50, 49)$.

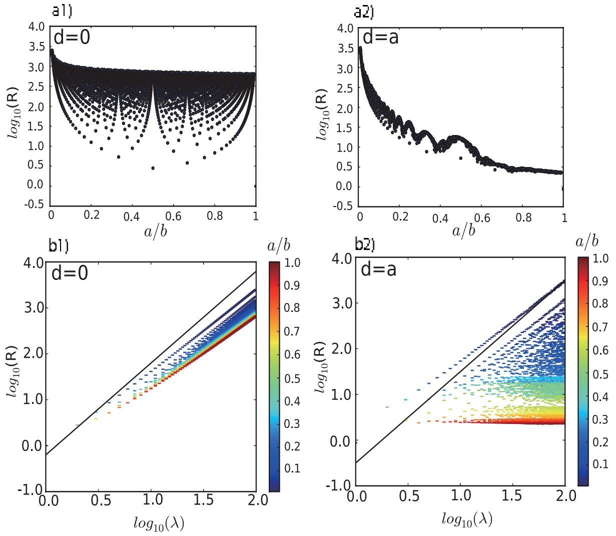

FIG. 6: The maximum value of the resistance R in the range of $0 \leq B_x ac \leq 2\pi$ as a function of $\frac{a}{b} = \frac{N_B}{N_A}$ for $d = 0$ ((a1)) and $d = a$ ((a2)), respectively. This complex relations are cleanly organized as a function of λ, which are shown in (b1) and (b2). The black solid lines are the guide to the eyes (slope 2) for the asymptotic relation $R \propto \lambda^2$.

surfaces. The maximum value of R changes radically in each n_A and n_B, which will be discussed later. R has the period from $b_x = 0$ to $b_x = 1$, and indicates a similar behavior to b_x for all (n_A, n_B) except for the even-odd effect. When either n_A or n_B is even, the b_x is shifted by $\frac{1}{2}$. b_x is the dimensionless magnetic flux penetrating the enlarged unit cell, which is scaled in an appropriate manner in each case as $B_x c\lambda = 2\pi b_x$. The larger λ becomes, R oscillates more rapidly as B_x. The panels (a1) and (b1) of Fig. 4 show R as a function of b_x, while (a2) and (b2) shows R as a function of $\frac{B_x ac}{2\pi}$. Panels (a1) and (a2) are for $(n_A, n_B) = (2, 1)$, while (b1) and (b2) are for $(n_A, n_B) = (50, 49)$. If λ become bigger, the resistivity R oscillate as $\frac{B_x ac}{2\pi}$ more rapidly.

Next, we consider a finite $d = a$. The behavior of the resistance R is not determined only by the parity of n_A and n_B, but it is different in each n_A and n_B because of the interference term F. The periodicity of R changes from $\Delta b_x = 1$ to $\Delta b_x = 2l_{AB}$, but the b_x-value at which $R = 0$ remains unchanged from the case of $d = 0$. The panels (a1) and (b1) of Fig. 5 show R as a function of b_x, while (a2) and (b2) as a function of $\frac{B_x ac}{2\pi}$. Panels (a1) and (a2) are for $(n_A, n_B) = (2, 1)$, while (b1) and (b2) are for $(n_A, n_B) = (50, 49)$. In the similar way to the case of $d = 0$, the larger λ become, the R oscillates as b_x changes of the order of 1 and hence more rapidly as a function of $\frac{B_x ac}{2\pi}$.

Establishing the enhanced magnetoresistance by λ, we next discuss the maximum value of the resistance $R_{\max}$ in the region $0 \leq B_x ac \leq 2\pi$. $R_{\max}$ indicates a singular behavior as a function of $\frac{a}{b} = \frac{N_B}{N_A}$ in (a1) and (a2) of Fig. 6 for two cases $d = 0$ and $d = a$, respectively. Both show the rather complex and singular behavior, but these are neatly organized as a function of λ as shown in (b1) and (b2) of Fig. 6. When $d \to 0$ (((b1)), $R_{\max}$ increases as λ as expected for all the regions of a/b (asymptotically λ^2 in the large λ limit). For $d = a$ (((b2)), on the other hand, $R_{\max}$ stays almost constant and independent of λ for $a \cong b$, while it approaches to the behavior of $d = 0$ as a/b decreases.

Now we discuss about the relevance of the present results to real systems. The disorder effect at the interface gives the mean free path ℓ. When the size λ of the enlarged unit cell is larger than ℓ, the singular dependence on a/b is broadened. In other words, the enhancement of the magnetoresistance saturates by the factor $\sim$min$(\ell, \lambda)^2$. The most relevant case to the real systems is that $a \cong b$ and $d \cong a$. In this case, the scale of the resistance R per unit area does not sensitively depends on the ratio a/b, while the magnetoresistance is determined by λ and depends strongly on the ratio a/b in a singular way. The essence of the enhanced magnetoresistance is the sensitive change in the interference pattern of the wavefunctions within the enlarged unit cell induced by the magnetic flux, it is expected that the magnetic field perpendicular to the interface also gives the similar effect to the parallel case discussed in the present paper.

In summary, we have studied the magentoresistance at the interface with misfit of lattice constants. We found that resistance R depends on the ratio a/b of the two lattice constants in a singular way, and the size λ of the enlarged unit cell determines the magnitude of the magnetoresistnce, which can he enhanced orders of magnitudes when a/b is a (nearly) irrational number.

The authors acknowledge the fruitful discussion with Y. Kawaguchi, K. Burch, M.Kawasaki and Y.Tokura. This work is supported by Grant-in-Aid for Scientific Research (Grants No. 24224009) from the Ministry of Education, Culture, Sports, Science and Technology of Japan, Strategic International Cooperative Program (Joint Research Type) from Japan Science and Technology Agency, and Funding Program for World-Leading Innovative RD on Science and Technology (FIRST Program).

---

detail calculations of Eq. (3)

In this appendix, we show detail calculations of Eq. (3). We write Eq. (1) by wave-number representation as

$$t_{kp} = \frac{1}{\sqrt{N_A N_B}} \sum_{nm} t_{nm} e^{-i\frac{2\pi k}{N_A}n + i\frac{2\pi p}{N_B}m} \tag{11}$$

$$= \frac{t_{AB}}{\sqrt{N_A N_B}} \sum_{nm} e^{-i\frac{2\pi n}{N_A}(k-M) + i\frac{2\pi m}{N_B}(p+M)} \left(e^{-\frac{L}{L_{AB}d}|n_B n - n_A m|} + e^{-\frac{L}{d} + \frac{L}{L_{AB}d}|n_B n - n_A m|} \right) \tag{12}$$

,where we use $a = \frac{1}{n_A}\frac{L}{G_{AB}}$ and $b = \frac{1}{n_B}\frac{L}{G_{AB}}$. At first, we decompose the summations into n_A and n_B parts by G_{AB},

$$t_{kp} = \frac{t_{AB}}{\sqrt{N_A N_B}} \sum_{m_A m_B=0}^{G_{AB}-1} \sum_{x=0}^{n_A-1} \sum_{y=0}^{n_B-1} e^{-\frac{L}{L_{AB}d}|n_A n_B(m_A - m_B) + n_B x - n_A y| - i\frac{2\pi(n_A m_A + x)}{N_A}(k-M) + i\frac{2\pi(n_B m_B + y)}{N_B}(p+M)} \tag{13}$$

$$+ \frac{t_{AB}}{\sqrt{N_A N_B}} \sum_{m_A, m_B=0}^{G_{AB}-1} \sum_{x=0}^{n_A-1} \sum_{y=0}^{n_B-1} e^{-\frac{L}{d} + \frac{L}{L_{AB}d}|n_A n_B(m_A - m_B) + n_B x - n_A y| - i\frac{2\pi(n_A m_A + x)}{N_A}(k-M) + i\frac{2\pi(n_B m_B + y)}{N_B}(p+M)}. \tag{14}$$

We define $y_- = \max\{y : n_B x > n_A y\}$ and rearrange the order of the summations, which begins at y_-, by making use of periodicity. It is specified as

$$t_{kp} = \frac{t_{AB}}{\sqrt{N_A N_B}} \sum_{m_A=0}^{G_{AB}-1} \sum_{x=0}^{n_A-1} \sum_{y=0}^{N_B-1} e^{-\frac{L}{L_{AB}d}(n_A(y + y_- + 1) - n_B x) - i\frac{2\pi(m_A n_A + x)}{N_A}(k-M) + i\frac{2\pi(m_A n_B + y_- + 1 + y)}{N_B}(p+M)} \tag{15}$$

$$+ \frac{t_{AB}}{\sqrt{N_A N_B}} \sum_{m_A=0}^{G_{AB}-1} \sum_{x=0}^{n_A-1} \sum_{y=0}^{N_B-1} e^{-\frac{L}{d} - \frac{L}{L_{AB}d}(n_B x - n_A(y + 1 + y_-)) - i\frac{2\pi(m_A n_A + x)}{N_A}(k-M) + i\frac{2\pi(m_A n_B + y_- + 1 + y)}{N_B}}. \tag{16}$$

Here, the summations over m_A and y is easily carried out. t_{kp} becomes

$$t_{kp} = t_{AB} \frac{\delta_{G_{AB}}(k - p - 2M)}{\sqrt{n_A n_B}} \frac{1 - e^{-\frac{L}{d}}}{1 - e^{-\frac{L n_A}{L_{AB}d} + i\frac{2\pi}{N_B}(p+M)}} \sum_{x=0}^{n_A-1} e^{-\frac{L}{L_{AB}d}(n_A(y_- + 1) - n_B x) - i\frac{2\pi x}{N_A}(k-M) + i\frac{2\pi(y_- + 1)}{N_B}(p+M)} \tag{17}$$

$$- t_{AB} \frac{\delta_{G_{AB}}(k - p - 2M)}{\sqrt{n_A n_B}} \frac{1 - e^{-\frac{L}{d}}}{1 - e^{\frac{L n_A}{M_{AB}d} + i\frac{2\pi}{N_B}(p+M)}} \sum_{x=0}^{n_A-1} e^{-\frac{L}{L_{AB}d}(n_B x - n_A(1 + y_-)) - i\frac{2\pi x}{N_A}(k-M) + i\frac{2\pi(y_- + 1)}{N_B}(p+M)}. \tag{18}$$

We define l as $l = \frac{L}{L_{AB}} = \frac{b}{n_A} = \frac{a}{n_B}$. y_- is equal to the quotient of $n_B x$ divided by n_A. We denote the remainder as Δx, i.e., $n_B x = n_A y_- + \Delta_x$. We write t_{kp} by Δx and $k - p - 2M = nG_{AB}$,

$$t_{kp} = t_{AB} \frac{\delta_{G_{AB}}(k - p - 2M)}{\sqrt{n_A n_B}} \frac{1 - e^{-\frac{L}{d}}}{1 - e^{-\frac{b}{d} + i\frac{2\pi}{N_B}(p+M)}} e^{-\frac{b}{d} + i\frac{2\pi}{N_B}(p+M)} \sum_{x=0}^{n_A-1} e^{-i\frac{2\pi x}{n_A}n + \left(\frac{l}{d} - i\frac{2\pi}{L_{AB}}(p+M)\right)\Delta x} \tag{19}$$

$$- t_{AB} \frac{\delta_{G_{AB}}(k - p - 2M)}{\sqrt{n_A n_B}} \frac{1 - e^{-\frac{L}{d}}}{1 - e^{\frac{b}{d} + i\frac{2\pi}{N_B}(p+M)}} e^{\frac{b}{d} + i\frac{2\pi}{N_B}(p+M)} \sum_{x=0}^{n_A-1} e^{-i\frac{2\pi x}{n_A}n - \left(\frac{l}{d} + i\frac{2\pi}{L_{AB}}(p+M)\right)\Delta x}. \tag{20}$$

We define x_A and x_B as solutions of the Diophantine equation, which is expressed as

$$n_B x_A - n_A x_B = 1. \tag{21}$$

This equation has a integer solution because n_A and n_B are coprime. The general solutions of this equation is represented as $(x_A + mn_A, x_B + mn_B)$, where m is an arbitrary integer. Thus $X_A = \Delta x x_A + mn_A$ and $X_B = \Delta x x_B + mn_B$ are satisfied with

$$n_B X_A - n_A X_B = \Delta x. \tag{22}$$

There is one-to-one correspondence between $x = 0, 1 \cdots n_A - 1$ and $\Delta x = 0, 1 \cdots n_A - 1$ because n_A and n_B are coprime. Δx is represented as $\Delta x = \Delta x x_A + mn_A$ where m is dependent on x. The summation over x is transformed into the summation over Δx,

$$t_{kp} = t_{AB} \frac{\delta_{G_{AB}}\left(k - p - 2M\right)}{\sqrt{n_A n_B}} \frac{1 - e^{-\frac{L}{d}}}{1 - e^{-\frac{b}{d} + i\frac{2\pi}{N_B}(p+M)}} e^{-\frac{b}{d} + i\frac{2\pi}{N_B}(p+M)} \sum_{\Delta x = 0}^{n_A - 1} e^{\left(\frac{l}{d} - i\frac{2\pi}{L_{AB}}(p+M) - i\frac{2\pi n}{n_A}x_A\right)\Delta x} \tag{23}$$

$$- t_{AB} \frac{\delta_{G_{AB}}\left(k - p - 2M\right)}{\sqrt{n_A n_B}} \frac{1 - e^{-\frac{L}{d}}}{1 - e^{\frac{b}{d} + i\frac{2\pi}{N_B}(p+M)}} e^{\frac{b}{d} + i\frac{2\pi}{N_B}(p+M)} \sum_{\Delta x = 0}^{n_A - 1} e^{-\left(\frac{l}{d} + i\frac{2\pi}{L_{AB}}(p+M) + i\frac{2\pi n}{n_A}x_A\right)\Delta x}. \tag{24}$$

After the summation over Δx and some calculations, t_{kp} become

$$t_{kp} = t_{AB} \frac{\delta_{G_{AB}}\left(k - p - 2M\right)}{\sqrt{n_A n_B}} \left(1 - e^{-\frac{L}{d}}\right) \frac{\sinh\left(\frac{l}{d}\right)}{\cosh\left(\frac{l}{d}\right) - \cos\left(\frac{2\pi}{L_{AB}}\left(p + M\right) + \frac{2\pi n}{n_A}x_A\right)}. \tag{25}$$

Eq. (3) is given by arranging Eq. 25 into the symmetric form by using $k - p - 2M = nG_{AB}$, which is

$$t_{kp} = \frac{t_{AB}}{\sqrt{n_A n_B}} \delta_{G_{AB}}\left(k - p - 2M\right) \left(1 - e^{-\frac{L}{d}}\right) \frac{\sinh\left(\frac{l}{d}\right)}{\cosh\left(\frac{l}{d}\right) - \cos\left(\frac{2\pi x_A}{N_A}\left(k - M\right) - \frac{2\pi x_B}{N_B}\left(p + M\right)\right)}. \tag{26}$$

detail calculations of Eq. (6) and Eq. (7)

In this appendix, we show detail calculations of Eq. (6) and Eq. (7). We assume that the tunneling amplitude between two lattices is the multiple of two copies of Eq. (1). The wave-number representation of the tunneling amplitude also become the multiple of two copies of Eq. (3), because calculations can be carried out independently in x- and y-directions. It is specified as

$$t_{\mathbf{kp}} = t_{AB} \frac{f_{2D}\left(\boldsymbol{k} - \boldsymbol{M}, \boldsymbol{p} + \boldsymbol{M}\right)}{n_A n_B} \delta^2_{G_{AB}}\left(\boldsymbol{k} - \boldsymbol{p} - 2\boldsymbol{M}\right) \tag{27}$$

$$f_{2D}\left(\boldsymbol{k}, \boldsymbol{p}\right) = f\left(k_x, p_x\right) f\left(k_y, p_y\right) \tag{28}$$

$$\delta^2_{G_{AB}}\left(\boldsymbol{k} - \boldsymbol{p}\right) = \delta_{G_{AB}}\left(k_x - p_x\right) \delta_{G_{AB}}\left(k_y - p_y\right). \tag{29}$$

The conductance between two lattices is calculated from

$$G = \sum_{\boldsymbol{kp}} \left|t_{\boldsymbol{kp}}\right|^2 \delta\left(\epsilon_A\left(\frac{2\pi}{N_A}\boldsymbol{k}\right)\right) \delta\left(\epsilon_B\left(\frac{2\pi}{N_B}\boldsymbol{p}\right)\right). \tag{30}$$

$\epsilon_{A(B)}$ is the energy dispersion for lattice A(B), which are periodic by 2π. The Brillouin Zones are similarly decomposed into $n_A \times n_A$ parts and $n_B \times n_B$ parts by new wave-number conservations by translational symmetries by $\lambda \boldsymbol{e}_x$ and

$\lambda \boldsymbol{e}_y$. Eq. (30) is transformed into the more meaningful form by the following calculations.

$$\begin{aligned}
G =& \frac{t_{AB}^2}{n_A^2 n_B^2} \sum_{k_x,k_y=0}^{N_A-1} \sum_{p_x,p_y=0}^{N_B-1} \delta_{G_{AB}}^2 \left(\boldsymbol{k}-\boldsymbol{p}-2\boldsymbol{M}\right) \left|f_{2D}(\boldsymbol{k}-\boldsymbol{M},\boldsymbol{p}+\boldsymbol{M})\right|^2 \delta\left(\xi_A\left(\frac{2\pi}{N_A}\boldsymbol{k}\right)\right)\delta\left(\xi_B\left(\frac{2\pi}{N_B}\boldsymbol{p}\right)\right) \\
=& \frac{t_{AB}^2}{n_A^2 n_B^2} \sum_{n_x,n_y=0}^{n_A-1} \sum_{p_x,p_y=0}^{N_B-1} \left|f_{2D}(\boldsymbol{p}+\boldsymbol{M}+\boldsymbol{n}G_{AB},\boldsymbol{p}+\boldsymbol{M})\right|^2 \delta\left(\xi_A\left(\frac{2\pi}{N_A}\left(\boldsymbol{n}G_{AB}+\boldsymbol{p}+2\boldsymbol{M}\right)\right)\right)\delta\left(\xi_B\left(\frac{2\pi}{N_B}\boldsymbol{p}\right)\right) \\
=& \frac{t_{AB}^2}{n_A^2 n_B^2} \sum_{n_x,n_y=0}^{n_A-1} \sum_{i_x,i_y=0}^{G_{AB}-1} \sum_{m_x,m_y=0}^{n_B-1} \left|f_{2D}(G_{AB}\boldsymbol{m}+\boldsymbol{i}+\boldsymbol{M}+G_{AB}\boldsymbol{n},G_{AB}\boldsymbol{m}+\boldsymbol{i}+\boldsymbol{M})\right|^2 \\
&\times \delta\left(\xi_A\left(\frac{2\pi}{N_A}\left(G_{AB}\boldsymbol{n}+G_{AB}\boldsymbol{m}+\boldsymbol{i}+2\boldsymbol{M}\right)\right)\right)\delta\left(\xi_B\left(\frac{2\pi}{N_B}\left(G_{AB}\boldsymbol{m}+\boldsymbol{i}\right)\right)\right) \\
=& \frac{t_{AB}^2}{n_A^2 n_B^2} \sum_{n_x,n_y=0}^{n_A-1} \sum_{i_x,i_y=0}^{G_{AB}-1} \sum_{m_x,m_y=0}^{n_B-1} \left|f_{2D}(G_{AB}\boldsymbol{n}+\boldsymbol{i}+\boldsymbol{M},G_{AB}\boldsymbol{m}+\boldsymbol{i}+\boldsymbol{M})\right|^2 \\
&\times \delta\left(\xi_A\left(\frac{2\pi}{N_A}\left(G_{AB}\boldsymbol{n}+\boldsymbol{i}+2\boldsymbol{M}\right)\right)\right)\delta\left(\xi_B\left(\frac{2\pi}{N_B}\left(G_{AB}\boldsymbol{m}+\boldsymbol{i}\right)\right)\right) \\
=& \frac{G_{AB}^2}{n_A^2 n_B^2} \sum_{n_x,n_y=0}^{n_A-1} \sum_{m_x,m_y=0}^{n_B-1} \sigma_{\boldsymbol{nm}}^{n_A n_B}(\boldsymbol{M})
\end{aligned}$$

with

$$\sigma_{\boldsymbol{kp}}^{n_A n_B}(\boldsymbol{M}) = \frac{t_{AB}^2}{G_{AB}^2} \sum_{i_x,i_y=0}^{G_{AB}-1} \left|f_{2D}(G_{AB}\boldsymbol{k}+\boldsymbol{i}+\boldsymbol{M},G_{AB}\boldsymbol{p}+\boldsymbol{i}+\boldsymbol{M})\right|^2 \delta\left(\xi_A\left(G_{AB}\boldsymbol{k}+\boldsymbol{i}+2\boldsymbol{M}\right)\right)\delta\left(\xi_B\left(G_{AB}\boldsymbol{p}+\boldsymbol{i}\right)\right) \tag{31}$$

Here, we take a limit $G_{AB} \to \infty$. Each term is replaced by $\frac{2\pi}{G_{AB}}\boldsymbol{i} \to 2\pi\boldsymbol{x}$ and $\frac{4\pi}{G_{AB}}\boldsymbol{M} \to 2\pi\boldsymbol{b}$,

$$\sigma_{\boldsymbol{kp}}^{n_A n_B}(\boldsymbol{M}) \to \iint_{I^2} d^2\boldsymbol{x} F\left(\boldsymbol{k}+\boldsymbol{x}+\frac{\boldsymbol{b}}{2},\boldsymbol{p}+\boldsymbol{x}+\frac{\boldsymbol{b}}{2}\right)\delta\left(\xi_A\left(\frac{2\pi}{n_A}\left(\boldsymbol{k}+\boldsymbol{b}+\boldsymbol{x}\right)\right)\right)\delta\left(\xi_B\left(\frac{2\pi}{n_B}\left(\boldsymbol{p}+\boldsymbol{x}\right)\right)\right)$$

with

$$\begin{aligned}
F(\boldsymbol{k},\boldsymbol{p}) &= \left|t_{AB} f_C\left(k_x,p_x\right) f_C\left(k_y,p_y\right)\right|^2 \\
f_C\left(k,p\right) &= \frac{\sinh\left(\frac{l}{d}\right)}{\cosh\left(\frac{l}{d}\right)-\cos\left(\frac{2\pi x_A}{n_A}k-\frac{2\pi x_B}{n_B}p\right)} \\
I^2 &= [0,1]\times[0,1].
\end{aligned}$$

detail calculations of the concrete example

In this section, we calculate the conductivity of the concrete example, i.e., $\epsilon_{A(B)}\left(\boldsymbol{k}\right) = \cos k_x + \cos k_y$ and $b_y = 0$. The conductivity is calculated from

$$\sigma_{n_A n_B} = \sum_{k_x,k_y=0}^{n_A-1} \sum_{p_x,p_y=0}^{n_B-1} \iint_{I^2} d^2\boldsymbol{x} \frac{F\left(\boldsymbol{k}+\boldsymbol{x}+\frac{b_x\boldsymbol{e}_{\boldsymbol{x}}}{2},\boldsymbol{p}+\boldsymbol{x}+\frac{b_x\boldsymbol{e}_x}{2}\right)}{n_A^2 n_B^2}\delta\left(\epsilon_A\left(\frac{2\pi}{n_A}\left(\boldsymbol{k}+b\boldsymbol{e}_x+\boldsymbol{x}\right)\right)\right)\delta\left(\epsilon_B\left(\frac{2\pi}{n_B}\left(\boldsymbol{p}+\boldsymbol{x}\right)\right)\right).$$

The calculation is done by the simple and straightforward method. We carry on the delta functions by the rule

$$\delta\left(g\left(x\right)\right) = \sum_i \frac{\delta\left(x-x_i\right)}{\left|g'\left(x_i\right)\right|} \tag{32}$$

one by one, where x_i is the ith zero point of $g(x)$. The result is

$$\sigma_{n_A n_B} = \frac{1}{4\pi^2 n_A n_B} \sum_{k_x=0}^{n_A-1} \sum_{p_x=0}^{n_B-1} \left(G\left(2k_x, 2p_x\right) + G\left(2k_x+1, 2p_x+1\right)\right) \tag{33}$$

$$G\left(k_x, p_x\right) = \frac{F\left(\frac{k_x+\Delta}{2}, \frac{p_x+\Delta}{2}, \frac{k_x+\Delta-n_A+b_x}{2}, -\frac{p_x+\Delta-n_B+b_x}{2}\right)}{\left|\sin\left(\frac{\pi}{n_A}\left(k_x+b_x+\Delta\right)\right)\sin\left(\frac{\pi}{n_B}\left(p_x-b_x+\Delta\right)\right)\right|} \tag{34}$$

with $\Delta = \frac{n_A+n_B}{2} - \left\lfloor \frac{n_A+n_B}{2} \right\rfloor$. In the limit $d \to 0$, The conductivity is summarized into the simpler form as

$$\sigma_{n_A n_B} = \frac{1}{2\pi^2 n_A n_B} \sum_{k_x=0}^{n_A-1} \sum_{p_x=0}^{n_B-1} \frac{1}{\left|\sin\left(\frac{\pi}{n_A}\left(k_x+\Delta+b_x\right)\right)\sin\left(\frac{\pi}{n_B}\left(p_x+\Delta-b_x\right)\right)\right|} \tag{35}$$

[1] H.Y. Hwang et al., Nat. Mat. **11(2)**, 103 (2012).
[2] A. Ohtomo, and H. Y. Hwang, Nature **427(6973)**, 423 (2004).
[3] J.S. Moodera et al., Phys. Rev. Lett. **74**, 3273 (1995).
[4] P. Bak, Rep. Prog. Phys. **45**, 587 (1982).
[5] J.B. Sokoloff, Phys. Rep. **126**, 189 (1985).
[6] E.L. Albuquerque, and M.G. Cottam, Phys. Rep. **376**, 225 (2003).